DOAJ
OPEN
GLOBAL
TRUSTED

SUPPORT ♡ ⌄   APPLY ⌄   SEARCH 🔍

SEARCH ⌄   DOCUMENTATION ⌄   ABOUT ⌄   LOGIN →
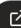
Feedback

International Journal on Smart Material and Mechatronics
IJSMM

📖 **2356-5314 (PRINT)**

[⧉ Website] [⧉ ISSN Portal]

About   Articles

PUBLISHING WITH THIS JOURNAL   **BEST PRACTICE**   **JOURNAL METADATA**

INDEX COPERNICUS
INTERNATIONAL   ICI World of Journals   ICI Journals Master List   ICI World of Papers

Deposited publications: 0 › Full text: 0% | Abstract: 0% | Keywords: 0% | References: 0%   Issues and contents

Journal description   Details   Scientific profile   **Editorial office**   Publisher

Metrics

Editor-in-Chief:	Assoc. Prof Rafiuddin Syam *Hasanuddin University* *Indonesia*
Editor:	Professor Mitsuhiro Okayasu *Okayama University* *Japan*
Editor:	Professor Keigo Watanabe *Okayama University* *Japan*
Editorial address:	Engineering Faculty Jl. P. Kemerdekaan Km 10 Makassar 90245 Makassar tel: +62411586015 E-mail: ijsmm14@gmail.com

Finite Element Analysis for Active-force Control on Vibration of a Flexible Single-link Manipulator

Abdul Kadir Muhammad[1)] and Shingo Okamoto[2)] and Jae Hoon Lee[2)]

[1)]Center for Mechatronics and Control Systems
Mechanical Engineering Department, State Polytechnic of Ujung Pandang, Makassar, Indonesia
[2)]Mechanical Engineering Department, Graduate School of Science and Engineering
Ehime University Matsuyama, Japan
Email: kadir.muhammad@poliupg.ac.id

Abstract— **The purposes of this research are to formulate the equations of motion of the system, to develop computational codes by a finite element analysis in order to perform dynamics simulation with vibration control, to propose an effective control scheme using active-force (AF) control a flexible single-link manipulator. The system used in this paper consists of an aluminum beam as a flexible link, a clamp-part, a servo motor to rotate the link and a piezoelectric actuator to control vibration. Computational codes on time history responses, FFT (Fast Fourier Transform) processing and eigenvalues-eigenvectors analysis were developed to calculate dynamic behavior of the link. Furthermore, the AF control was designed to drive the piezoelectric actuator. Calculated results have revealed that the vibration of the system can be suppressed effectively.**

Index Terms— **Active-force control, finite element analysis, flexible manipulator, piezoelectric actuator, vibration control.**

I. INTRODUCTION

Employment of flexible link manipulator is recommended in the space and industrial applications in order to accomplish high performance requirements such as high-speed besides safe operation, increasing of positioning accuracy and lower energy consumption, namely less weight. However, it is not usually easy to control a flexible manipulator because of its inheriting flexibility. Deformation of the flexible manipulator when it is operated must be considered by any control. Its controller system should be dealt with not only its motion but also vibration due to the flexibility of the link.

The purposes of this research are to formulate the equations of motion of the system, to develop computational codes by a finite element analysis in order to perform dynamics simulation with vibration control, to propose an effective control scheme using active-force (AF) control a flexible single-link manipulator.

The system used in this paper consists of an aluminum beam as a flexible link, a clamp-part, a servo motor to rotate the link and a piezoelectric actuator to control vibration. Computational codes on time history responses, FFT (Fast Fourier Transform) processing and eigenvalues-eigenvectors analysis were developed to calculate dynamic behavior of the link. Furthermore, the AF control was designed to drive the piezoelectric actuator. It was done by adding bending moments generated by the piezoelectric actuator to the single-link.

II. FORMULATION BY FINITE ELEMENT METHOD

The link has been discretized by finite-elements. The finite-element has two degrees of freedom, namely the lateral deformation $v(x,t)$, and the rotational angle $\psi(x,t)$ [1 − 4]. The length, the cross-sectional area and the area moment of inertia around z-axis of every element are denoted by l_i, S_i and I_{zi} respectively. Mechanical properties of every element are denoted as Young's modulus E_i and mass density ρ_i.

A. Kinematics

Fig. 1 shows the position vector $\boldsymbol{r}$ of an arbitrary point P in the link in the global and rotating coordinate frames. Let the link as a flexible beam has a motion that is confined in the horizontal plane as shown in figure 1. The $O - XY$ frame is the global coordinate frame while $O - xy$ is the rotating coordinate frame fixed to the root of the link. The unit vectors in X, Y, x and y axes are denoted by $\boldsymbol{I}$, $\boldsymbol{J}$, $\boldsymbol{i}$ and $\boldsymbol{j}$, respectively. A motor is installed on the root of the link. The rotational angle of the motor when the link rotates is denoted by $\theta(t)$.

The position vector $\boldsymbol{r}(x,t)$ of the arbitrary point P in the link at time $t = t$, measured in the $O - XY$ frame shown in figure 1 is expressed by
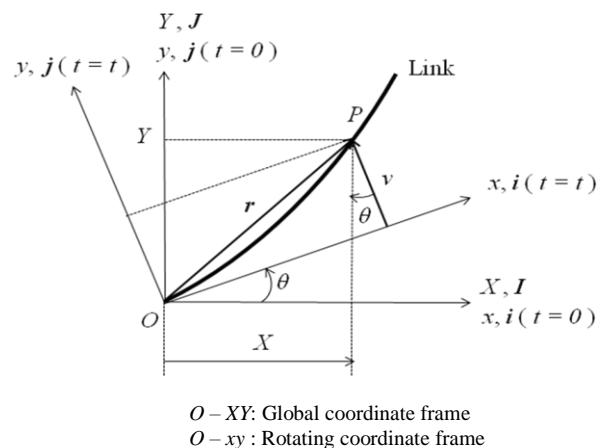
$$\boldsymbol{r}(x,t) = X(x,t)\boldsymbol{I} + Y(x,t)\boldsymbol{J} \tag{1}$$

O − XY: Global coordinate frame
O − xy : Rotating coordinate frame

Fig. 1. Position vector of an arbitrary point *P* in the link in the global and rotating coordinate frames

International Journal on Smart Material and Mechatronics Vol. 2 No. 2 2015
Abdul Kadir Muhammad, State Polytechnik of Ujung Pandang, Indonesia

p-ISSN: 2356-5314
e-ISSN: 2460-075X

where

$$X(x,t) = x\cos\theta(t) - v(t)\sin\theta(t) \qquad (2)$$

$$Y(x,t) = x\sin\theta(t) + v(t)\cos\theta(t) \qquad (3)$$

The velocity vector of P at time $t = t$ is given by

$$\dot{r}(x,t) = \dot{X}(x,t)\boldsymbol{I} + \dot{Y}(x,t)\boldsymbol{J} \qquad (4)$$
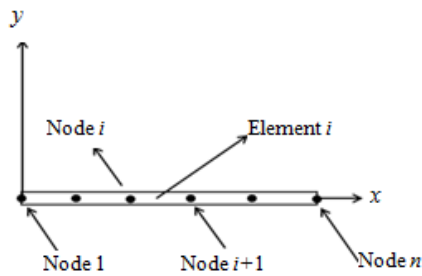
B. Finite Element Procedure

Figure 2 shows the rotating coordinate frame and the link divided by one-dimensional and two-node elements. Then, Fig. 3 shows the element coordinate frame of the *i-th* element. Here, there are four boundary conditions together at nodes i and (i+1). The four boundary conditions are expressed as nodal displacement vector as follow

$$\boldsymbol{\delta}_i = \{v_i \quad \psi_i \quad v_{i+1} \quad \psi_{i+1}\}^T \qquad (5)$$
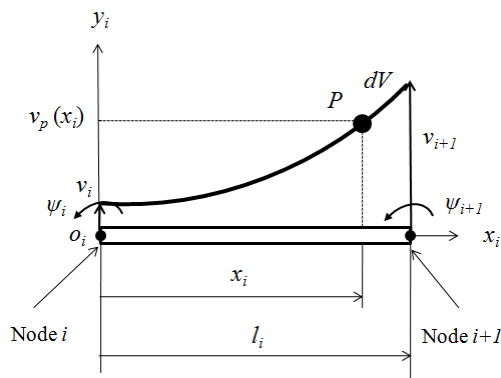
Then, the hypothesized deformation has four constants as follows [7]

$$v_i = a_1 + a_2 x_i + a_3 x_i^{\,2} + a_4 x_i^{\,3} \qquad (6)$$

$o - xy$: Rotating coordinate frame

Fig. 2. Rotating coordinate frame and the link divided by the one-dimensional and two-node elements

$o_i - x_i y_i$: Element coordinate frame of the *i*-th element

Fig. 3. Element coordinate frame of the *i-th* element

The relation between the lateral deformation v_i and the rotational angle ψ_i of the node i is given by

$$\psi_i = \frac{\partial v_i}{\partial x_i} \qquad (7)$$

Furthermore, from mechanics of materials, the strain of node i can be defined by

$$\varepsilon_i = -y_i \frac{\partial^2 v_i}{\partial x_i^{\,2}} \qquad (8)$$

C. Equations of Motion

Equation of motion of the i-th element is given by

$$\boldsymbol{M}_i \ddot{\boldsymbol{\delta}}_i + \boldsymbol{C}_i \dot{\boldsymbol{\delta}}_i + \left[\boldsymbol{K}_i - \dot{\theta}^2(t)\boldsymbol{M}_i\right]\boldsymbol{\delta}_i = \ddot{\theta}(t)\boldsymbol{f}_i \qquad (9)$$

where $\boldsymbol{M}_i$, $\boldsymbol{C}_i$, $\boldsymbol{K}_i$, $\ddot{\theta}(t)\boldsymbol{f}_i$ are the mass matrix, damping matrix, stiffness matrix and the excitation force generated by the rotation of the motor respectively. The representation of the matrices and vector in Eq. (9) can be found in [1]. Finally, the equation of motion of the system with n elements considering the boundary conditions is given by

$$\boldsymbol{M}_n \ddot{\boldsymbol{\delta}}_n + \boldsymbol{C}_n \dot{\boldsymbol{\delta}}_n + \left[\boldsymbol{K}_n - \dot{\theta}^2(t)\boldsymbol{M}_n\right]\boldsymbol{\delta}_n = \ddot{\theta}(t)\boldsymbol{f}_n \qquad (10)$$

III. MODELING

Figure 4 shows a model of the single-link manipulator, the clamp-part and the piezoelectric actuator. The link including the clamp-part and actuator were discretized by 35 elements. The clamp-part is more rigid than the link. Therefore Young's modulus of the clamp-part was set in 1,000 times of the link's. The piezoelectric actuator was bonded to a one-side surface of Element 4. A schematic representation on modeling of the piezoelectric actuator is shown in Fig. 5.
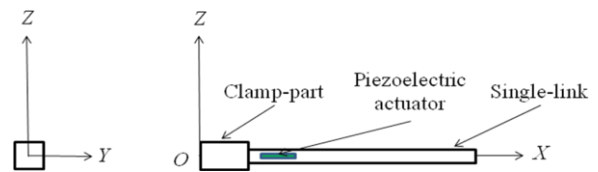

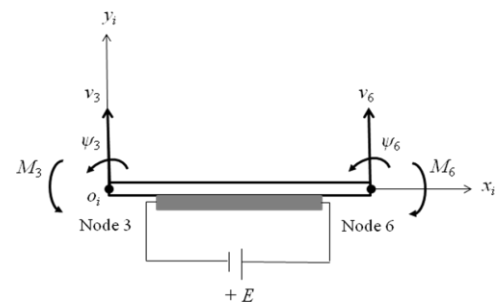Fig. 4. Computational model of the flexible single-link manipulator

Fig. 5. Modeling of the piezoelectric actuator

Furthermore, a strain gage was bonded to the position of Node 6 of the single-link (0.11 m from the origin). Physical parameters of the single-link model and the piezoelectric actuator are shown in table 1.

The piezoelectric actuator suppressed the vibration of the flexible link manipulator by adding bending moments at Nodes 3 and 6, M_3 and M_6 to the flexible link. The bending moments are generated by applying voltages E to the piezoelectric actuator as shown in Fig. 3. The relation between the bending moments and the voltages are related by

$$M_3 = -M_6 = d_1 E \qquad (11)$$

Here d_1 is a constant quantity.

Furthermore, the voltage to generate the bending moments is proportional to the strain ε of the single-link due to the vibration. The relation can be expressed as follows

$$E = \pm \frac{1}{d_2} \varepsilon \qquad (12)$$

Here d_2 is a constant quantity. Then, d_1 and d_2 will be determined by comparing the calculated results and experimental ones.

Computational codes were developed to perform dynamics simulation of the system based on the formulation that explained above. The validation was done using time history responses analysis of free vibration, natural frequencies using FFT (Fast Fourier Transform) processing, vibration modes and natural frequencies using eigenvalues-eigenvectors analysis and time history responses analysis due to the base excitation [1 – 4].

TABLE I

PHYSICAL PARAMETERS OF THE FLEXIBLE LINK AND THE PIEZOELECTRIC ACTUATOR [14]

l : Total length	m	3.91×10^{-1}
l_l : Length of the link	m	3.50×10^{-1}
l_c : Length of the clamp-part	m	4.10×10^{-2}
l_a : Length of the actuator	m	2.00×10^{-2}
S_l : Cross section area of the link	m²	1.95×10^{-5}
S_c : Cross section area of the clamp-part	m²	8.09×10^{-4}
S_a : Cross section area of the actuator	m²	1.58×10^{-5}
I_{zl} : Cross section area moment of inertia around z-axis of the link	m⁴	2.75×10^{-12}
I_{zc} : Cross section area moment of inertia around z-axis of the clamp-part	m⁴	3.06×10^{-8}
I_{za} : Cross section area moment of inertia around z-axis of the actuator	m⁴	1.61×10^{-11}
E_l : Young's Modulus of the link	GPa	7.03×10^{1}
E_c : Young's Modulus of the clamp-part	GPa	7.00×10^{4}
E_a : Young's Modulus of the actuator	GPa	4.40×10^{1}
ρ_l : Density of the link	kg/m³	2.68×10^{3}
ρ_c : Density of the clamp-part	kg/m³	9.50×10^{2}
ρ_a : Density of the actuator	kg/m³	3.33×10^{3}
α : Damping factor of the link	-	2.50×10^{-4}

IV. CONTROL SCHEME

A control scheme to suppress the vibration of the single-link was designed using the piezoelectric actuator. It was done by adding bending moments generated by the piezoelectric actuator to the single-link. Therefore, the equation of motion of the system become

$$M_n \ddot{\delta}_n + C_n \dot{\delta}_n + \left[K_n - \dot{\theta}^2(t) M_n \right] \delta_n = \ddot{\theta}(t) f_n + u_n(t) \qquad (13)$$

where the vector $u_n(t)$ containing M_3 and M_6 is the control force generated by the actuator to the single-link.

To drive the actuator, AF control has been designed and examined.

Fig. 5 shows the block diagram of the AF control that is proposed in this research. In this strategy, vibration of the system is controlled by canceling bending moments acting at Nodes 3 and 6 due to the base excitation (excitation bending moments). The following steps are the way to estimate and cancel the excitation bending moments.

Firstly, the strain, ε_6 at Node 6 is measured to estimate the lateral deformation, v_6 at the Node 6. The relation between the strain and the lateral deformation considering the boundary conditions can be defined as follows

$$\frac{v_6}{\varepsilon_6} = -\frac{x^2(x-3l)}{6y(x-l)} = A \qquad (14)$$

where l, x and y are the length of the link, the position of Node 6 in x and y directions, respectively.

Secondly, the actual force in the s-domain acting at Node 6 can be defined in the form of the Newton's equation of motion as follows

$$F_6(s) = M_{ii(i=11)} s^2 v_6 \qquad (15)$$

where $M_{ii(i=11)}$ is the component of the mass matrix corresponding to v_6.

Thirdly, the bending moments acting at Nodes 3 and 6 are estimated using the following equation
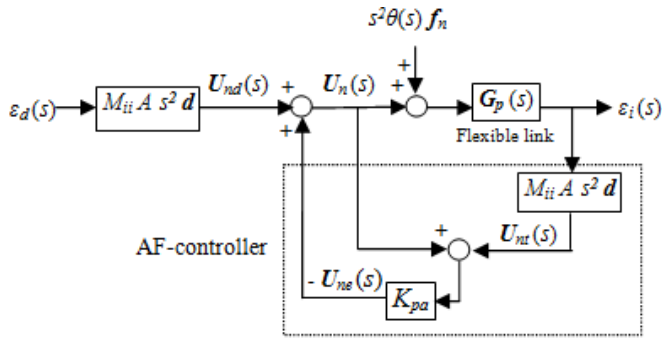
$$U_{nt}(s) = \pm F_6(s) d \qquad (16)$$

The vector d that represents the position vector from the reference point to the position where the excitation force acting can be written as follows

$$d = \left\{ 0 \quad 0 \quad 0 \quad l_2 \quad 0 \quad l_2 \quad 0 \quad \cdots \quad 0 \right\}^T \qquad (17)$$

Fourthly, based on Fig. 6, the excitation bending moments can be calculated as

$$U_{ne}(s) = K_{pa} \left\{ U_{nt}(s) - U_n(s) \right\} \qquad (18)$$

where K_{pa} is the non-dimensional proportional gain of the proposed AF control.

ε_d: Desired strain ε_i: Measured strains at Node i
θ: Rotation angle of the motor M_{ii}: Component of mass matrix
A: Conversion from ε_i to v_i d: Position vector
U_{nd}: Desired bending moments U_n: Applied bending moments
U_{ne}: Excitation bending moments U_{nt}: Bending moments

Fig. 6. Block diagram of active-force control of the flexible link manipulator

Finally, the bending moments applying as a control force to control the vibration of the system can be calculated as follows

$$U_n(s) = -U_{ne}(s) + U_{nd}(s) \qquad (19)$$

where $U_{nd}(s)$ is the desired bending moments which is zero. The negative of $U_{ne}(s)$ indicates that the bending moments used to cancel the vibration of the system.

V. CALCULATED RESULTS

Time history responses of strains on the uncontrolled and controlled systems were calculated when the motor rotated by the angle of $\pi/2$ radians (90 degrees) within 0.68 [s]. Time history responses of strains on uncontrolled and controlled systems were calculated for the model under the control scheme as shown in Fig. 6.
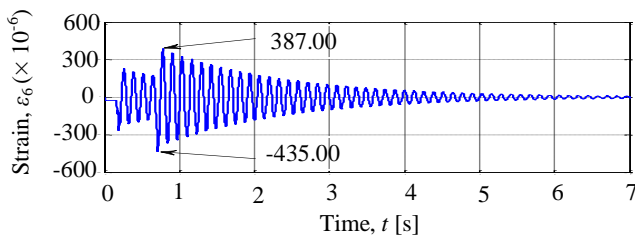
(a)   Uncontrolled system
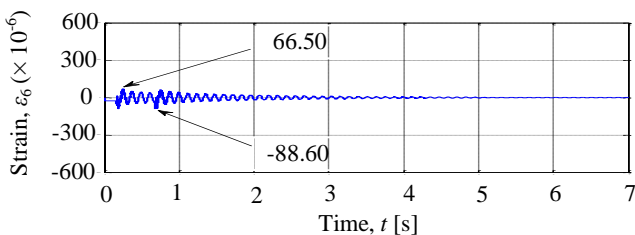
(b)   Controlled by AF-controller, K_{pa} = 0.4 [-]

Fig.7. Calculated time history responses of strains at Node 6 for uncontrolled and controlled system due to the base excitation

Examining several gains of the AF controller leaded to K_{pa} = 0.4 [-] as the better one. Figure 7 shows the uncontrolled and controlled time history responses of strains at Node 6. The maximum and minimum strains of uncontrolled system in positive and negative sides were 387.00×10^{-6} and -435.00×10^{-6}, as shown in Fig. 7(a). By using AF-controller they became 66.50×10^{-6} and -88.60×10^{-6}, as shown in Fig. 7(b).

VI. CONCLUSIONS

The equations of motion for the flexible single-link manipulator had been derived using the finite element method. Computational codes had been developed in order to perform dynamic simulations of the system. Calculated results on time history responses, natural frequencies and vibration modes show the validities of the formulation, computational codes and modeling of the system. The active-force (AF) control was designed to suppress the vibration of the system. The calculated results show the effectiveness of the proposed AF control to suppress the vibration of the flexible single-link manipulator.

REFERENCES

[1] A.K. Muhammad, S. Okamoto and J.H. Lee, "Computer Simulations on Vibration Control of a Flexible Single-link Manipulator Using Finite-element Method", Proceeding of 19th International Symposium of Artificial Life and Robotics, 2014, pp. 381 – 386.

[2] A.K. Muhammad, S. Okamoto and J.H. Lee, "Computer Simulations and Experiments on Vibration Control of a Flexible Link Manipulator Using a Piezoelectric Actuator", Lecture Notes in Engineering and Computer Science: Proceeding of The International MultiConference of Engineers and Computer Scientists 2014, IMECS 2014, pp. 262 – 267.

[3] A.K. Muhammad, S. Okamoto and J.H. Lee, "Comparison of Proportional-derivative and Active-force Controls on Vibration of a Flexible Single-link Manipulator Using Finite-element Method", Journal of Artificial Life and Robotics, Vol. 19. No. 4, 2014, pp. 375 – 381.

[4] A.K. Muhammad, S. Okamoto and J.H. Lee, "Comparison of Proportional and Active-force Controls on Vibration of a Flexible Link Manipulator Using a Piezoelectric Actuator through Calculations and Experiments", Engineering Letters, Vol. 22. No.3, 2014, pp. 134 – 141.

[5] A.K. Muhammad, S. Okamoto and J.H. Lee, "Computational Simulations on Vibration Control of a Flexible Two-link Manipulator by Piezoelectric Actuator Using Finite Element Method", Proceeding of Asia-Pacific Conference on Engineering and Applied Sciences, 2015, pp. 173 – 188.

[6] A.K. Muhammad, S. Okamoto and J.H. Lee, "Computational Simulations and Experiments on Vibration Control of a Flexible Two-link Manipulator Using a Piezoelectric Actuator", Engineering Letters, Vol. 23. No.3, 2015, pp. 200 – 209.

[7] M. Lalanne, P. Berthier and J.D. Hagopian, Mechanical Vibration for Engineers, John Wiley & Sons Ltd, 1983, pp. 146 – 153.

[8] www.mmech.com, Resin Coated Multilayer Piezoelectric Actuators.